

# Experimental application of Takagi-Sugeno observers and controllers in a nonlinear electromechanical system

Zsófia Lendek\* Antonio Sala\*\* Pedro García\*\* Roberto Sanchis\*\*\*

\* *Department of Automation, Technical University of Cluj-Napoca, Memorandumului 28, 400114 Cluj-Napoca, Romania*

*zsofia.lendek@aut.utcluj.ro.*

\*\* *Universidad Politécnica de Valencia, 46020 Valencia, Spain.*

*{asala,pggil}@isa.upv.es*

\*\*\* *Universitat Jaume I, 12071 Castelló de la Plana, Spain.*

*rsanchis@esid.uji.es*

---

**Abstract:** In this paper, a systematic methodology to design fuzzy Takagi-Sugeno observers and controllers will be used to estimate the angular positions and speeds, as well as to stabilise an experimental mechanical system with 3 degrees of freedom (fixed quadrotor). Takagi-Sugeno observers and controllers are compared to observers and controllers based on the linearized model, both designed with the same optimization criteria and design parameters. Experimental results confirm that Takagi-Sugeno models and observers behave similarly to linear ones around the linearization point, but have a better performance over a larger operating range, as intuitively expected.

**Keywords:** Takagi-Sugeno (T-S) fuzzy model, Observer-based control, Linear matrix inequalities (LMIs), Experimental application.

---

## 1. INTRODUCTION

Takagi-Sugeno (Takagi and Sugeno, 1985) fuzzy models are able to exactly represent a complex dynamic system by interpolating the behaviour of several LTI (Linear Time Invariant) submodels (Lee et al., 2001; Tanaka et al., 1998). Also, approximately, such models may be obtained by blending linearizations in several operation points (Tanaka and Wang, 2001; Zhang and Zeng, 2012). TS models are currently being used for a large class of physical and industrial processes, in a wide range of application areas (Abdelazim and Malik, 2005; Liu, 2007; Marx et al., 2007; Lendek et al., 2010b; Hidayat et al., 2010).

The linear matrix inequality (LMI, (Boyd et al., 1994)) framework allows designing controllers and observers for such TS fuzzy systems (Tanaka and Wang, 2001; Lendek et al., 2010a; Guelton et al., 2012), as well as static output feedback ones (Dong and Yang, 2007). The reader is referred to (Feng, 2006; Sala et al., 2005; Sala, 2009) for ample reference on the achievements and perspectives of fuzzy control.

In particular, the design of state observers for non-linear systems using TS models has been actively considered during the last decades (Benhadj and Rotella, 1995; Lendek et al., 2010d). Observers for TS systems are easily developed in the case of measurable premise variables: several types of observers have been developed for TS fuzzy systems, among which: fuzzy Thau-Luenberger observers (Tanaka et al., 1998),

reduced-order observers (Bergsten et al., 2002), and sliding-mode observers (Palm and Bergsten, 2000). These observers are designed such that the estimation error dynamics are asymptotically stable. In general, the design methods lead to an LMI feasibility problem, for which efficient algorithms exist. Unmeasurable premise variables present more difficulties and limitations; some results in such a case are reported in (Guerra et al., 2006; Lendek et al., 2010d,c; Tanaka et al., 2011).

This paper presents the design of a fuzzy TS observer and a controller for an electromechanical system with 3 degrees of freedom (a 3DoF fixed quadrotor from Quanser<sup>®</sup>). Its first-principle rigid-body model is nonlinear and nonlinearities also arise in the propeller. The problem dealt with in this work is related to rigid-body attitude control (Marcu, 2011), although the fixed 3DoF setup makes it a different one to the full 6DoF problem and allows for a different, more complete, instrumentation (particularly encoders). Hence, the proposed system may be a sensible benchmark for nonlinear control and observation techniques. As nonlinearities around the equilibrium point are smooth, modelling and control can be carried out by using nonlinear Takagi-Sugeno (TS) models.

The resulting observer and controller are *experimentally* tested, and their performance is compared with a linear observer and controller designed in a similar manner (i.e., with the same LMIs and performance criteria).

In order to accomplish the design goals, the techniques in (Lendek et al., 2010b) (observers) and (Wu and Cai, 2006) (guaranteed-cost control) have been refined and adapted to the particular application problem in consideration.

---

\* The work of Zs. Lendek was supported by a grant of the Romanian National Authority for Scientific Research, CNCS-UEFISCDI, project number PN-II-RU-TE-2011-3-0043, contract number 74/05.10.2011. Spanish authors are grateful to grants DPI2011-27845-C02-01 (A. Sala), DPI2011-27845-C02-02 (R. Sanchis), DPI2011-28507-C02-01 (P. Garcia) from Spanish Government, and PROMETEOII/2013/004 (A. Sala, P. Garcia) from Generalitat Valenciana.

The contributions of this paper are, first, formalising a discrete-time disturbance-rejection LMI for observers with unmeasurable premises and proposing a simple improvement to the methodology to obtain a bound on some uncertain term appearing in the error dynamics; second, exploring in detail its adaptation to the 3DoF electromechanical quadrotor model and experimentally assessing the possible advantages with respect to a linearised output-feedback controller when closing the loop with a robust guaranteed-cost controller. In (Lendek et al., 2011), a preliminary conference version of part of the work was outlined. Here, the procedure to compute the observer mismatch term later denoted as  $\mu$  and a closed-loop robust fuzzy guaranteed-cost control have been developed, with the experiments to illustrate its performance.

The paper is organized as follows: Section 2 presents the sector nonlinearity approach that will be used for obtaining the TS representation of the quadrotor's model and conditions for observer and controller design. The platform and the mathematical model of the quadrotor are described in Section 3. The TS modeling of the quadrotor is realized in Section 4, the observers are designed in Section 5 and the controller design is shown in Section 6. Section 7 presents experimental results and, finally, Section 8 provides some conclusions.

## 2. PRELIMINARIES: TS MODELS, OBSERVERS AND CONTROLLERS

Consider a non-linear system

$$\begin{aligned} x[k+1] &= f(\rho[k])x[k] + g(\rho[k])u[k] \\ y[k] &= Cx[k] \end{aligned} \quad (1)$$

with  $f$  and  $g$  smooth non-linear matrix functions,  $x \in \mathcal{R}^n$  the state vector,  $u \in \mathcal{R}^{n_u}$  the input vector,  $y \in \mathcal{R}^{n_y}$  the measurement vector,  $\rho[k]$  some vector function of  $x$ ,  $y$ , and  $u$ , denoted in literature as ‘‘premise’’ or ‘‘scheduling’’ vector. All variables are assumed to be bounded on a compact set  $\mathcal{C}_{xyu}$ . In the so-called Takagi-Sugeno systems and controllers, the premise vector usually includes elements of the state  $x$ , as follows.

*Takagi-Sugeno Models.* The sector-nonlinearity technique can be applied to the above system in order to obtain a so-called TS model. Basically, following (Tanaka and Wang, 2001; Ohtake et al., 2001), let  $\text{nl}_j(\cdot) \in [\underline{\text{nl}}_j, \overline{\text{nl}}_j]$ ,  $j = 1, 2, \dots, p$  be the set of bounded non-linearities in  $f$  and  $g$ , i.e., components of either  $f$  or  $g$ . An exact TS fuzzy representation of (1) can be obtained by constructing first the weighting functions

$$w_0^j(\cdot) = \frac{\overline{\text{nl}}_j - \text{nl}_j(\cdot)}{\overline{\text{nl}}_j - \underline{\text{nl}}_j} \quad w_1^j(\cdot) = 1 - w_0^j(\cdot) \quad (2)$$

for each nonlinearity  $j = 1, 2, \dots, p$ , and defining the so-called *membership functions* as

$$h_i(\rho[k]) = \prod_{j=1}^p w_{i_j}^j(\rho_j[k]) \quad (3)$$

with  $i = 1, 2, \dots, 2^p$ ,  $i_j \in \{0, 1\}$ . These membership functions are normal, i.e.,

$$\sum_{i=1}^r h_i(\rho[k]) = 1 \quad h_i(\rho[k]) \geq 0, \quad i = 1, 2, \dots, r$$

and  $r = 2^p$ , where  $r$  is the number of rules. For instance,  $\text{nl}_1(x) = \sin(x)$  can be expressed in the interval  $[-2, 2]$  as an interpolation  $\sin(x) \equiv w_0^1(x) \cdot (1 \cdot x) + w_1^1(x) \cdot (\sin(2)/2 \cdot x)$ .

Using the membership functions defined in (3), an exact representation of (1) is given as:

$$\begin{aligned} x[k+1] &= \sum_{i=1}^r h_i(\rho[k])(A_i x[k] + B_i u[k]) \\ y[k] &= Cx[k] \end{aligned} \quad (4)$$

with  $r$  the number of local linear models,  $A_i$  and  $B_i$  matrices of proper dimensions, with  $i = 1, 2, \dots, r$ , and  $h_i$  defined as in (3). The reader is referred to (Tanaka and Wang, 2001) for ample detail on TS modelling.

*TS observers.* In general, an observer designed for the model (4) has the form

$$\begin{aligned} \hat{x}[k+1] &= \sum_{i=1}^r h_i(\hat{\rho}[k]) \left( A_i \hat{x}[k] + B_i u[k] + L_i (y[k] - \hat{y}[k]) \right) \\ \hat{y}[k] &= C\hat{x}[k] \end{aligned} \quad (5)$$

where  $\hat{\rho}$  denotes the estimated scheduling vector and  $L_i$ ,  $i = 1, \dots, r$ , are the observer gains. The observer design problem is to calculate the values of  $L_i$  such that the estimation error converges to zero. Approaches to TS observer designs in literature have been considered in (Lendek et al., 2010b, 2009, 2010e).

For the particular case in which all  $B_i$  are equal, the dynamics of the estimation error,  $e[k] = x[k] - \hat{x}[k]$ , are given by (Lendek et al., 2010d):

$$\begin{aligned} e[k+1] &= \sum_{i=1}^r h_i(\hat{\rho}[k]) (A_i - L_i C) e[k] \\ &\quad + \sum_{i=1}^r (h_i(\rho[k]) - h_i(\hat{\rho}[k])) (A_i x[k]) \end{aligned} \quad (6)$$

If the memberships derivatives are continuous, there exists a  $\mu > 0$  so that for all  $k$ ,

$$\left\| \sum_{i=1}^r (h_i(\rho[k]) - h_i(\hat{\rho}[k])) A_i x[k] \right\| \leq \mu \|e[k]\| \quad (7)$$

i.e., the last term in (6) tends to zero as  $\hat{\rho}[k]$  approaches  $\rho[k]$ . The Appendix will discuss a variation in order to obtain the smallest possible bound  $\mu$ .

Inspired by the developments in (Lendek et al., 2010d) using the above bound, the estimation error dynamics (6) is asymptotically stable if there exists a positive definite matrix  $P$  and generic matrices  $M_i$  such that (Hidayat et al., 2010) the LMIs below hold:

$$\begin{pmatrix} P - \mu^2 I & * & * \\ PA_i - M_i C & P & * \\ 0 & P & I \end{pmatrix} > 0 \quad i = 1, \dots, r \quad (8)$$

Once the solution is found, the observer gains are  $L_i = P^{-1}M_i$ . Section 5 will present a more general result involving disturbance-rejection bounds.

*TS controller.* As discussed in the introduction, in the literature many proposals exist for controlling TS systems. In the present quadrotor application a guaranteed-cost (GC) control strategy has been tested. Some GC proposals appear in (Wu and Cai, 2004; Tanaka et al., 2009); in (Ariño et al., 2010) state and input constraints are considered (resulting, however, in an iterative non-LMI procedure).

The following discrete-time fuzzy model with parameter uncertainties (9) has been considered (Wu and Cai, 2006) for control design:

$$\begin{aligned}
x[k+1] &= \sum_{i=1}^r h_i(\rho[k])(A_i x[k] + \Delta A_i[k]) \\
&\quad + (B_i + \Delta B_i[k])u[k], \quad x(0) = x_0 \quad (9) \\
z[k] &= \sum_{i=1}^r h_i(\rho[k])C_i x[k] + D_i u[k]
\end{aligned}$$

where  $\Delta A_i[k]$  and  $\Delta B_i[k]$  represent the time-varying parametric uncertainties of the system, having the following structure:

$$(\Delta A_i[k] \ \Delta B_i[k]) = HF[k](E_{1i} \ E_{2i}) \quad (10)$$

where  $F[k]$  is an unknown time-varying matrix that satisfies:

$$F[k]^T F[k] \leq I \quad (11)$$

The terms  $H$ ,  $E_{1i}$ , and  $E_{2i}$  of (10) are known constant matrices with appropriate dimensions that specify how the uncertain parameters in  $F[k]$  affect the nominal matrices  $A_i$  and  $B_i$ , see (Wu and Cai, 2006).

Define the performance index as follows:

$$J = \sum_{k=1}^{\infty} z^T[k]z[k] \quad (12)$$

The objective of the control design is to obtain the lowest-possible guaranteed upper bound for  $J$  for an initial state lying in a prescribed region (defined below with a quadratic inequality). This strategy is denoted in literature as guaranteed-cost (GC) control.

Consider now a so-called parallel-distributed compensator (PDC) controller widely used in literature as:

$$u = \sum_{i=1}^r h_i(\rho[k])K_i x[k] \quad (13)$$

where  $K_i \in \mathbb{R}^{m \times n}$ ,  $i = 1, \dots, r$  are feedback gain matrices to be determined. The chosen control design technique in the application in this paper is based on the result below:

*Theorem 1.* ((Wu and Cai, 2006)). If there exist a common matrix  $X > 0$ , matrices  $Y_j$ ,  $j \in \mathbb{S}$  and a scalar  $\varepsilon > 0$  satisfying the following LMIs:

$$\begin{aligned}
\Psi_{ii} &< 0, \quad i = 1, \dots, r \\
\Psi_{ij} + \Psi_{ji} &< 0, \quad i < j, \quad i, j = 1, \dots, r, \\
\begin{bmatrix} Z & * \\ U & X \end{bmatrix} &> 0
\end{aligned} \quad (14)$$

where  $\Psi_{ij}$  is given by

$$\Psi_{ij} \triangleq \begin{bmatrix} -X & 0 & 0 & A_i X + B_i Y_j & \varepsilon H \\ * & -\varepsilon I & 0 & E_{1i} X + E_{2i} Y_j & 0 \\ * & * & -I & C_i X + D_i Y_j & 0 \\ * & * & * & -X & 0 \\ * & * & * & * & -\varepsilon I \end{bmatrix} \quad (15)$$

then there exists a fuzzy controller (13) such that the closed-loop fuzzy system is quadratically stable and the performance index satisfies

$$J \leq \text{trace}\{Z\} \quad (16)$$

for all admissible parameter uncertainties if the initial state is in the set

$$\Omega_0 = \{x_0 \mid x_0 = Uv, v^T v \leq 1\}$$

The state feedback gain matrices are given by

$$K_j = Y_j X^{-1}$$

By minimising the trace of  $Z$ , the optimal bound and its associated controller gains are obtained via convex optimization with well-known software tools.

Note that in the case of common  $B$ , which is true in our quadrotor model, only a single-sum expression has to be evaluated, as  $A_i X + B_i Y_j$  will be replaced by  $A_i X + B Y_i$ , and  $E_{1i} X + E_{2i} Y_j$  will change to  $E_{1i} X + E_{2i} Y_i$  (details omitted for brevity).

Of course, apart from the robust guaranteed-cost choice above, other possible controller design strategies from literature might also be used ( $\mathcal{H}_\infty$ ,  $\mathcal{L}_1$ , decay-rate or even combining several LMIs to set up a multicriteria approach (Zhang and Zeng, 2012)).

Note that, when implemented, the estimated state feedback

$$u = \sum_{i=1}^r h_i(\hat{\rho}[k])K_i \hat{x}[k]$$

will actually be used. If the initial conditions are close enough to the origin (so that, in the transient, the state does not exit the region in which the bound  $\mu$  has been computed in (7)) the observer LMIs ensure  $\hat{x} \rightarrow x$  and  $\hat{\rho} \rightarrow \rho$  and input-to-state argumentations would ensure stability (see also (Bergsten, 2001; Tanaka et al., 2011)). Theoretical determination of such initial domain of attraction with low conservativeness is a matter of current research, but the methodologies in this section have proved successful in the practical application this paper describes.

### 3. DESCRIPTION OF EXPERIMENTAL PLATFORM

This section describes the physical plant to be controlled, the computing platform and the nonlinear model.

*Controlled process.* The experimental platform chosen to evaluate the performance of the designed fuzzy control is a three degrees of freedom (3DOF) system (Quanser, 2011). The hardware platform, shown in Figure 1, consists in a quadrotor mounted on a 3 DOF pivot joint, such that the body can freely move in roll, pitch, and yaw. The sensors of the platform are encoders that measure the position of the three orientation-axes of the quadrotor  $\phi$ ,  $\theta$ , and  $\psi$ . With the available sensors, the angular velocities cannot be measured. The control inputs are the voltages  $V_1$ ,  $V_2$ ,  $V_3$ , and  $V_4$  applied to the 4 propellers of the quadrotor.

*Computing platform.* A PC running Linux-RT, a soft RTOS distributed with a GNU GPLv2 license is provided to implement the control algorithms, on top of an Ubuntu installation. The communications between the PC and the quadrotor platform were made with a PMC I/O target. Linux RT is a Linux O.S. with a patch whose objective is to minimize the amount of kernel code that is nonpreemptible. In this way, faster sampling periods with more reliable real-time guarantees (reduced sampling period jitter) can be implemented. The controller has been implemented in C++, using the newmat matrix library available in Ubuntu repositories. With the above operating system and an Intel I3 processor at 3.3 GHz, the computing power was ample enough to execute the fuzzy observation and control loop with a sampling period of 5 ms.

*Nonlinear model.* The non-linear model of the platform is presented in the following equations, as given in (Bouabdallah, 2007) from approximating the Euler equations of motion:

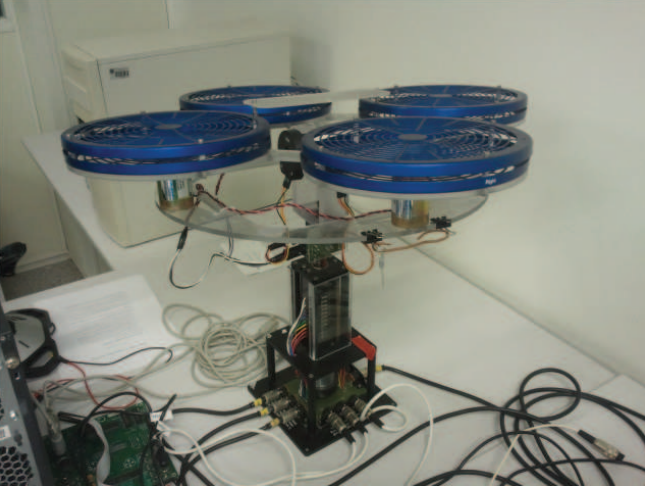


Figure 1. The Quanser<sup>®</sup> quad-rotor 3DoF system.

$$\begin{aligned}\ddot{\phi} &= \frac{J_r \dot{\theta}}{I_{xx}} K_v (V_1 + V_3 - V_2 - V_4) + \frac{I_{yy} - I_{zz}}{I_{xx}} \dot{\theta} \dot{\psi} + u_1 \\ \ddot{\theta} &= \frac{J_r \dot{\phi}}{I_{xx}} K_v (-V_1 - V_3 + V_2 + V_4) + \frac{I_{zz} - I_{xx}}{I_{yy}} \dot{\psi} \dot{\phi} + u_2 \\ \ddot{\psi} &= \frac{I_{xx} - I_{yy}}{I_{zz}} \dot{\theta} \dot{\phi} + u_3\end{aligned}\quad (17)$$

where each acceleration input ( $u_1$ ,  $u_2$ ,  $u_3$ ) depends on the applied voltages as follows:

$$\begin{aligned}u_1 &= \frac{b l K_v^2 (V_2^2 - V_4^2)}{I_{xx}} \\ u_2 &= \frac{b l K_v^2 (V_3^2 - V_1^2)}{I_{yy}} \\ u_3 &= \frac{d K_v^2 (V_1^2 - V_2^2 + V_3^2 - V_4^2)}{I_{zz}}\end{aligned}\quad (18)$$

from the nonlinear propellers' actuation<sup>1</sup> approximately proportional to the square of the rotor speed (in turn, to the input voltage). The symbols used and their values in physical units, where applicable, are given in Table 1 (extracted from the manufacturer's documentation in (Quanser, 2011)).

For observer design purposes, in what follows, the input signals will be considered to be the transformed signals  $u_i$ . A suitable inversion will be made to compute the actual voltages in closed-loop control (see later).

The input voltages  $V_i$ ,  $i = 1, 2, 3, 4$ , are limited by the drivers,  $V_i \in [V_{\min}, V_{\max}]$ , with  $V_{\min} = -10\text{V}$  and  $V_{\max} = 10\text{V}$ . We considered that the angular velocities  $\dot{\phi}$ ,  $\dot{\theta}$ ,  $\dot{\psi}$  are bounded,  $\dot{\phi}$ ,  $\dot{\theta}$ ,  $\dot{\psi} \in [d\alpha_{\min}, d\alpha_{\max}]$ , with  $d\alpha_{\min} = -\pi/4$  rad/s and  $d\alpha_{\max} = \pi/4$  rad/s. The maximum pitch and roll angles are assumed to be  $\pi/2$  rad, while the maximum yaw angle is also  $\pi$  rad.

#### 4. DISCRETE TS MODELING OF THE 3DOF QUADROTOR

In this section an exact TS representation of the discretized 3DOF model is developed. The TS model will be used later to design the non-linear observer and state-feedback controller for the quadrotor system.

<sup>1</sup> The square is shorthand for  $\text{sign}(V_i)V_i^2$  to account for upwards and downwards thrust.

Table 1. Quadrotor variables and parameters

Symbol	Meaning	Type	Units
$\phi$	Roll angle	Measured	rad
$\dot{\phi}$	Roll angular velocity	Estimated	rad/s
$\theta$	Pitch angle	Measured	rad
$\dot{\theta}$	Pitch angular velocity	Estimated	rad/s
$\psi$	Yaw angle	Measured	rad
$\dot{\psi}$	Yaw angular velocity	Estimated	rad/s
$V_i$	Voltage applied to propeller $i$	Known input	V
$K_v$	Transformation constant	54.945	rad s/V
$J_r$	Rotators inertia	$6 \cdot 10^{-5}$	kgm <sup>2</sup>
$I_{xx}$	Inertia X-axis	0.0552	kgm <sup>2</sup>
$I_{yy}$	Inertia Y-axis	0.0552	kgm <sup>2</sup>
$I_{zz}$	Inertia Z-axis	0.1104	kgm <sup>2</sup>
$b$	Thrust coefficient	$3.935139 \cdot 10^{-6}$	N/Volt
$d$	Drag coefficient	$1.192464 \cdot 10^{-7}$	Nm/Volt
$l$	Distance from pivot to motor	0.1969	m
$m$	Mass	2.85	kg
$g$	Acceleration due to gravity	9.81	m/s <sup>2</sup>
$T_s$	Sampling time	0.005	s

The gyroscopic effects in the roll and pitch dynamics contain the term  $K_v(V_1 + V_3 - V_2 - V_4)$ , which is the sum of the (known) inputs. This term is denoted by

$$u_g = K_v(V_1 + V_3 - V_2 - V_4)$$

Furthermore, to simplify the notations, the terms containing the moments of inertia of the 3DOF quadrotor are denoted as  $I_{xyz} = \frac{I_{xx} - I_{yy}}{I_{zz}}$ ,  $I_{yzx} = \frac{I_{yy} - I_{zz}}{I_{xx}}$ , and  $I_{zxy} = \frac{I_{zz} - I_{xx}}{I_{yy}}$ .

With the notations presented above, the model (17) is rewritten as

$$\begin{aligned}\ddot{\phi} &= \frac{J_r \dot{\theta}}{I_{xx}} u_g + I_{yzx} \dot{\theta} \dot{\psi} + u_1 \\ \ddot{\theta} &= -\frac{J_r \dot{\phi}}{I_{xx}} u_g + I_{zxy} \dot{\psi} \dot{\phi} + u_2 \\ \ddot{\psi} &= I_{xyz} \dot{\theta} \dot{\phi} + u_3\end{aligned}\quad (19)$$

The state vector  $x$  is defined as  $x = (\phi, \dot{\phi}, \theta, \dot{\theta}, \psi, \dot{\psi})^T$ . Then, one possible<sup>2</sup> representation of (19) is

$$\begin{aligned}\dot{x} &= A_{cont}(x)x + B_c u \\ y &= Cx\end{aligned}$$

with model matrices

$$A_{cont}(x) = \begin{pmatrix} 0 & 1 & 0 & 0 & 0 & 0 \\ 0 & 0 & 0 & \frac{J_r}{I_{xx}} u_g & 0 & I_{yzx} x_4 \\ 0 & 0 & 0 & 1 & 0 & 0 \\ 0 & -\frac{J_r}{I_{xx}} u_g & 0 & 0 & 0 & I_{zxy} x_2 \\ 0 & 0 & 0 & 0 & 0 & 1 \\ 0 & I_{xyz} x_4 & 0 & 0 & 0 & 0 \end{pmatrix}$$

$$B_c = \begin{pmatrix} 0 & 0 & 0 \\ 1 & 0 & 0 \\ 0 & 0 & 0 \\ 0 & 1 & 0 \\ 0 & 0 & 0 \\ 0 & 0 & 1 \end{pmatrix}; \quad C = \begin{pmatrix} 1 & 0 & 0 & 0 & 0 & 0 \\ 0 & 0 & 1 & 0 & 0 & 0 \\ 0 & 0 & 0 & 0 & 1 & 0 \end{pmatrix}$$

where  $x_i$  denotes the  $i$ th variable of the state vector  $x$ .

Since the variables are measured in discrete time, with a sampling period of 5 ms, a discrete-time observer will be designed. It is assumed that the sampling period is small enough such

<sup>2</sup> Due to the multiplication of the angular velocities, the matrix  $A_{cont}(x)$  can be defined in several ways. This is a well-known fact, i.e., TS models are not unique and, sometimes, ones may be better than others (Sala, 2009).

that an Euler discretization can be effectively used for the model (19). Consequently, the non-linear discrete-time model is

$$\begin{aligned} x[k+1] &= A_d(x[k])x[k] + B_d u[k] \\ y[k] &= Cx[k] \end{aligned} \quad (20)$$

with discrete-time model matrices given by

$$A_d(x[k]) = \begin{pmatrix} 1 & T_s & 0 & 0 & 0 & 0 \\ 0 & 1 & 0 & T_s \frac{J_r}{I_{xx}} u_g[k] & 0 & T_s I_{yzx} x_4[k] \\ 0 & 0 & 1 & T_s & 0 & 0 \\ 0 & -T_s \frac{J_r}{I_{xx}} u_g[k] & 0 & 1 & 0 & T_s I_{zxy} x_2[k] \\ 0 & 0 & 0 & 0 & 1 & T_s \\ 0 & T_s I_{xyz} x_4[k] & 0 & 0 & 0 & 1 \end{pmatrix} \quad (21)$$

$$B_d = T_s B_c$$

To obtain an exact fuzzy representation of the non-linear model (20), the sector non-linearity approach (Ohtake et al., 2001) is used.

The non-constant terms in the matrix  $A_d(x[k])$  are  $u_g[k]$ ,  $x_4[k]$ , and  $x_2[k]$ , therefore  $z[k] = (u_g[k], x_2[k], x_4[k])^T$ . Each of these terms are bounded and their weighting functions are constructed as follows:

- (1) The bounds on the term  $u_g[k]$  can be computed based on the bounds of the voltage input and are  $u_{g,\min} = 4K_v V_{\min}$  and  $u_{g,\max} = 4K_v V_{\max}$ . The weighting functions are  $w_1^0 = \frac{u_{g,\max} - u_g[k]}{u_{g,\max} - u_{g,\min}}$  and  $w_1^1 = 1 - w_1^0$ . The term  $u_g[k]$  is expressed as  $u_g[k] = u_{g,\min} w_1^0 + u_{g,\max} w_1^1$ .
- (2) The bounds of  $x_4[k]$  are the bounds of the angular velocity,  $d\alpha_{\min}$  and  $d\alpha_{\max}$ . The weighting functions are  $w_2^0 = \frac{d\alpha_{\max} - x_4[k]}{d\alpha_{\max} - d\alpha_{\min}}$  and  $w_2^1 = 1 - w_2^0$ . The term  $x_4[k]$  is expressed as  $x_4[k] = d\alpha_{\min} w_2^0 + d\alpha_{\max} w_2^1$ .
- (3)  $x_2[k]$  is also angular velocity, and its bounds and weighting functions are the same as for  $x_4[k]$ . Thus, the weighting functions are  $w_3^0 = \frac{d\alpha_{\max} - x_2[k]}{d\alpha_{\max} - d\alpha_{\min}}$  and  $w_3^1 = 1 - w_3^0$ . The term  $x_2[k]$  is expressed as  $x_2[k] = d\alpha_{\min} w_3^0 + d\alpha_{\max} w_3^1$ .

As shown above, there are three non-linearities. For each of these nonlinearities we have 2 weighting functions, and therefore the fuzzy model will have  $2^3 = 8$  rules. The membership functions are computed as (3), and the corresponding local linear models are obtained by substituting the corresponding values into the  $A_d$  matrix. For instance, the first membership function and the corresponding consequent matrix are

$$h_1(z[k]) = w_1^0 w_2^0 w_3^0$$

$$A_1 = \begin{pmatrix} 1 & T_s & 0 & 0 & 0 & 0 \\ 0 & 1 & 0 & T_s \frac{J_r}{I_{xx}} u_{g,\min} & 0 & T_s I_{yzx} d\alpha_{\min} \\ 0 & 0 & 1 & T_s & 0 & 0 \\ 0 & -T_s \frac{J_r}{I_{xx}} u_{g,\min} & 0 & 1 & 0 & T_s I_{zxy} d\alpha_{\min} \\ 0 & 0 & 0 & 0 & 1 & T_s \\ 0 & T_s I_{xyz} d\alpha_{\min} & 0 & 0 & 0 & 1 \end{pmatrix}$$

**Remark:** Note that one of the premise variables in the fuzzy model depends on the control action ( $u_g$  depends on the propellers' speed). It is not a problem in the observer design, as it will assume  $u$  as known, but it will induce an algebraic loop in the controller implementation. In order to approximately solve it,  $u_g$  may be computed with the control action applied in the last sample. This is a reasonable solution as long as the sampling period and the difference between consecutive inputs is small enough and it has been the chosen option in this paper.

## 5. OBSERVER DESIGN

### 5.1 TS observer

In practice both the states and the measurements are corrupted by noise, i.e., the system equations will now be written as

$$\begin{aligned} x[k+1] &= \sum_{i=1}^r h_i(\rho[k]) (A_i x[k]) + Bu + Qv[k] \\ y[k] &= Cx[k] + R\eta[k] \end{aligned} \quad (22)$$

where  $v[k]$  and  $\eta[k]$  are the state transition noise (process noise) and measurement noise, respectively.

The fuzzy observer is defined as

$$\begin{aligned} \hat{x}[k+1] &= \sum_{i=1}^r h_i(\hat{\rho}[k]) (A_i \hat{x}[k] + L_i (y[k] - \hat{y}[k])) + Bu \\ \hat{y}[k] &= C\hat{x}[k] \end{aligned} \quad (23)$$

and, hence, the error dynamics – taking into account the disturbances – is given by:

$$\begin{aligned} e[k+1] &= \sum_{i=1}^r h_i(\hat{\rho}[k]) \left( (A_i - L_i C) e[k] + (Q - L_i R) \begin{pmatrix} v[k] \\ \eta[k] \end{pmatrix} \right) \\ &+ \sum_{i=1}^r (h_i(\rho[k]) - h_i(\hat{\rho}[k])) A_i x[k] \end{aligned} \quad (24)$$

with the observer-model mismatch assumed satisfying a Lipschitz condition:

$$\left\| \sum_{i=1}^r (h_i(\rho[k]) - h_i(\hat{\rho}[k])) A_i x[k] \right\| \leq \mu \|e[k]\| \quad (25)$$

*Lemma 1.* Consider the model (22). If, given  $\beta > 0$  the LMI optimization problem below is feasible for some  $P > 0$  and  $M_i$  decision variables:

$$\begin{pmatrix} \beta^2 P - \mu^2 I & * & * & * & * \\ 0 & \gamma I & * & * & * \\ 0 & 0 & I & * & * \\ PA_i - M_i C & PQ & -M_i R & P & P \\ D & 0 & 0 & 0 & \gamma I \end{pmatrix} > 0 \quad (26)$$

$\forall i = 1, \dots, r$

Then:

- (1) the obtained  $\gamma$  is a bound for the disturbance rejection performance, in induced 2-norm ( $\mathcal{H}_\infty$  in a linear case), i.e.:

$$\|De\|_2 \leq \gamma \|I\omega\|_2 \quad (27)$$

where  $D$  is an arbitrary user-defined weighing matrix,

- (2) a decay rate  $\beta$  – i.e., there exists a bound  $\zeta(e[0])$  such that  $\|e[k]\| \leq \zeta(e[0])\beta^k$  – would be achieved in the disturbance-free case.

**Proof.** Introducing the notation:

$$\begin{aligned} \xi[k] &= \sum_{i=1}^r (h_i(\rho[k]) - h_i(\hat{\rho}[k])) (A_i x[k]) \\ G_{\hat{\rho}} &= \sum_{i=1}^r (h_i(\hat{\rho}[k]) (A_i - L_i C)) \\ \omega[k] &= \begin{pmatrix} v[k] \\ \eta[k] \end{pmatrix} \\ M_{\hat{\rho}} &= \sum_{i=1}^r (h_i(\hat{\rho}[k]) (Q - L_i R)) \end{aligned} \quad (28)$$

the closed-loop error dynamics can be expressed as:

$$e[k+1] = G_{\hat{\rho}}e[k] + M_{\hat{\rho}}\omega[k] + \xi[k] \quad (29)$$

and we have, by (25):

$$\|\xi[k]\| \leq \mu\|e[k]\| \quad (30)$$

The disturbance rejection (27), multiplied by any arbitrary  $\tau > 0$ , can be equivalently expressed as:

$$\sum_{k=0}^{\infty} \begin{pmatrix} e[k] \\ \omega[k] \end{pmatrix}^T \begin{pmatrix} \gamma^{-1}\tau D^T D & 0 \\ 0 & -\gamma\tau I \end{pmatrix} \begin{pmatrix} e[k] \\ \omega[k] \end{pmatrix} \leq 0 \quad (31)$$

Also, proposing a Lyapunov function  $V[k] = e[k]^T P e[k]$ :

$$V[k+1] = (G_{\hat{\rho}}e[k] + M_{\hat{\rho}}\omega[k] + I\xi[k])^T P (G_{\hat{\rho}}e[k] + M_{\hat{\rho}}\omega[k] + I\xi[k]) \quad (32)$$

the well-known dissipation inequality may be stated:

$$V[k+1] - V[k] + e^T[k]\gamma^{-1}\tau D^T D e[k] - \gamma\tau\omega[k]^T \omega[k] < 0 \quad (33)$$

so, if  $V(0) = 0$ , for any final instant  $N$  we have:

$$\sum_{k=0}^N e^T[k]\gamma^{-1}\tau D^T D e[k] - \gamma\tau\omega[k]^T \omega[k] < 0 \quad (34)$$

and, hence, taking  $N \rightarrow \infty$ , we have (27).

Then, to take into account the bounding of the observer model mismatch (30), as S-procedure Lagrange multiplier  $\tau$  is introduced and the Lyapunov decrease  $V[k+1] - V[k]$  is changed to a decay-rate condition  $V[k+1] - V[k] \leq V[k+1] - \beta^2 V[k] < 0$ , resulting in:

$$V[k+1] - \beta^2 V[k] + \tau * ((e[k])^T \mu^2 I (e[k]) - \xi[k]^T I \xi[k]) + \begin{pmatrix} e[k] \\ \omega[k] \end{pmatrix}^T \begin{pmatrix} \gamma^{-1}\tau D^T D & 0 \\ 0 & -\gamma\tau I \end{pmatrix} \begin{pmatrix} e[k] \\ \omega[k] \end{pmatrix} < 0 \quad (35)$$

Defining now  $\kappa^T = (e[k]^T \ \omega[k]^T \ \xi[k]^T)$ , we have:

$$\kappa^T \begin{pmatrix} G_{\hat{\rho}}^T \\ G_{\hat{\rho}}^T \\ I \end{pmatrix} P P^{-1} P (G_{\hat{\rho}} \ M_{\hat{\rho}} \ I) \kappa + \kappa^T \begin{pmatrix} -\beta^2 P + \mu^2 \tau I + \gamma^{-1} \tau D^T D & 0 & 0 \\ 0 & -\gamma \tau I & 0 \\ 0 & 0 & -\tau I \end{pmatrix} \kappa < 0 \quad (36)$$

Assuming  $\tau = 1$ , with no loss of generality as  $P$  can be scaled also by  $\tau$ , and using Schur complement twice, we get:

$$\begin{pmatrix} -\beta^2 P + \mu^2 I & 0 & 0 & G_{\hat{\rho}}^T P & D^T \\ 0 & -\gamma I & 0 & M_{\hat{\rho}}^T P & 0 \\ 0 & 0 & -I & P & 0 \\ P G_{\hat{\rho}} & P M_{\hat{\rho}} & P & -P & 0 \\ D & 0 & 0 & 0 & -\gamma I \end{pmatrix} < 0 \quad (37)$$

and, replacing  $M_i = P L_i$  the LMI (26) in the lemma is readily obtained.

Note that the first condition would describe the ‘‘stationary’’ performance whereas the second one would bound the convergence rate in the initial instants of the observer operation where errors would be likely larger due to initial condition mismatch. Both performance measures are important in practice.

*Summary of observer design parameters.* The design parameters are:

- The process- and measurement-noise variances, Q and R, which are analogous to those in standard linear observer

design (such as those designed with  $\mathcal{H}_2$  –Kalman filter– or  $\mathcal{H}_{\infty}$  criteria).

- A multicriteria performance objective ( $\gamma$ : disturbance attenuation;  $\beta$ : decay rate). The most basic choice is  $\beta = 1$  and minimizing gamma.
- A ‘‘scaling’’ matrix D: as different state variables have different units, they must be scaled in order to be suitably compared. These scalings are widely used in multivariable control (Skogestad and Postlethwaite, 2007). Scaling  $D$  also allows focusing the desired error performance on a particular subset of the variables.

The rest of the elements are either model matrices or LMI decision variables found by the optimization software. Note that the Lipschitz constant  $\mu$  is obtained from the model (see Appendix).

In summary, the design parameters are not that different to what an ordinary linear observer design would need (disturbance sizes, scaling of the variables – diagonal weights –, optimization of the attenuation factor/pole region).

For this platform the process noise affects mainly the acceleration equations. Based on the properties of the platform, and on different experimental trials, the design parameters are:

$$\begin{aligned} Q &= \text{diag}(0.0001, 1, 0.0001, 1, 0.0001, 1) \\ R &= \text{diag}(8 \cdot 10^{-4}, 8 \cdot 10^{-4}, 8 \cdot 10^{-4}) \\ D &= \text{diag}(10, 0.038, 10, 0.038, 10, 0.038) \\ \beta &= 1 \\ \mu &= 0.03 \end{aligned}$$

The selected  $\beta = 1$  indicates that only disturbance-rejection performance is actually desired.

The methodology for the calculation of  $\mu$  is given in Appendix. The result, with the values of the platform, and bounding the angular velocity of the quadrotor to 28 degree/s, give a minimum  $\mu = 0.03$ . As it will be seen in Section 7.1, even though the theory does not assure higher velocities, in the experiment, the results show a better performance of the TS observer in a range of angular velocities exceeding the theoretically proved one.

In total 8 observer gains have been obtained by solving (26). For instance, the gain matrix for the first rule is:

$$L_{TS,1} = \begin{pmatrix} 1.1799 & 0.0000 & -0.0000 \\ 35.9791 & -0.4295 & 0.1508 \\ -0.0000 & 1.1799 & 0.0000 \\ 0.4299 & 35.9791 & -0.1509 \\ 0.0000 & -0.0000 & 1.1918 \\ 0.0001 & -0.0002 & 38.3548 \end{pmatrix}$$

The numerical values of the other seven gains obtained by the LMI solver have been omitted for brevity.

## 5.2 Linear observer

In order to compare with a standard non-fuzzy design, a linear observer is designed on the same criteria as the TS one.

To design this observer, first the non-linear model, presented in (21), is linearised around  $x = 0$ , obtaining

$$\begin{aligned} x[k+1] &= A_0 x[k] + B_d u[k] + v[k] \\ y[k+1] &= C x[k+1] + \eta[k] \end{aligned} \quad (38)$$

where  $A_0$  is the state matrix linearised at  $x = 0$ ,  $B_d$  is the input matrix,  $C$  is the measurement matrix, and  $v[k]$  and  $\eta[k]$  have the same interpretation as in (22).

A deterministic linear observer is considered. The resulting equation is:

$$\hat{x}[k+1] = A_0\hat{x}[k] + B_d u[k] + L_L(y[k] - C\hat{x}[k])$$

where  $L_L$  denotes the observer gain. This gain is computed by solving the matrix inequality (26), similarly to the TS observer design (considering  $\mu = 0$ ).

The obtained single linear gain is:

$$L_L = \begin{pmatrix} 1.0509 & -0.0000 & -0.0000 \\ 10.1863 & -0.0000 & -0.0000 \\ -0.0000 & 1.0509 & 0.0000 \\ -0.0000 & 10.1863 & 0.0000 \\ -0.0000 & 0.0000 & 1.0509 \\ -0.0000 & 0.0000 & 10.1863 \end{pmatrix}$$

Hence, the linear observer uses only one observer gain and one model whereas the TS one interpolates between eight gains and eight models.

The difference in the values of the observer gains can be explained by the effect that  $\mu$  has on the LMI of the TS: as expected, a more uncertain ‘‘state equation’’ results in higher sensor-to-state gains to compensate for uncertainty with higher-gain feedback.

The obtained values for  $\gamma$  are 124.1009 for the TS observer and 107.7917 for the linear observer. As expected, the linear observer (one model) obtains a better bound in the vicinity of the origin than the TS observer which takes into account nonlinearities: it is easier to observe a single process than a nonlinear combination of eight of them. Note, however, that as the linear process is subject to a substantially larger modelling error, experimental performance away from the linearization point will not be better than the TS one even if the ideal  $\gamma$  might make think that (see experiment section).

## 6. CONTROLLER DESIGN

In general, for TS systems with unmeasured premise variables, the separation principle at the large does not hold. However, as long as the initial conditions are sufficiently close to the origin, and the trajectories do not exceed the largest Lyapunov level set, stability is ensured (see (Bergsten, 2001; Tanaka et al., 2011)). In this paper, to specifically account for the mismatch introduced by the observer, we use a robust controller. Thus, the design of the state feedback gain has incorporated modelling errors, in order to approximately take into account both the unmodelled plant dynamics regarding control and the difference  $x - \hat{x}$  from the observer.

In particular, the matrices  $E$  and  $H$  are set up to incorporate uncertainty in the equations governing the angular speed computations. Hence, the proposed output equation of the controlled variable  $z$ , with different state and input weights, and the uncertainty matrices are, in Matlab-like notation:

$$\begin{aligned} C &= [\text{blkdiag}(3, 0.65, 3, 0.65, 6, 1.3); \text{zeros}(3, 6)] \\ D &= [\text{zeros}(6, 3); \text{blkdiag}(0.03, 0.03, 0.03)] \\ H &= \begin{bmatrix} 0 & 1 & 0 & 0 & 0 & 0 \\ 0 & 0 & 0 & 1 & 0 & 0 \\ 0 & 0 & 0 & 0 & 0 & 1 \end{bmatrix}^T \\ E_{1i} &= T_s \cdot [H \cdot \eta_1; \text{zeros}(3, 6)] \\ E_{2i} &= T_s \cdot [\text{zeros}(3, 3); \eta_2 \cdot I] \end{aligned} \quad (39)$$

where  $\eta_1 = 0.2$  and  $\eta_2 = 0.2$  are the magnitude of the uncertainties in the angular speed and actuators, respectively, obtained based on the values from Table 1, multiplying a matrix  $F[k]$  of size  $3 \times 6$  in (11). In this way the uncertainty structure yields:

$$\Delta A_i = \begin{pmatrix} 0 & 0 & 0 & 0 & 0 & 0 \\ 0 & f_{11} & 0 & f_{12} & 0 & f_{13} \\ 0 & 0 & 0 & 0 & 0 & 0 \\ 0 & f_{21} & 0 & f_{22} & 0 & f_{23} \\ 0 & 0 & 0 & 0 & 0 & 0 \\ 0 & f_{31} & 0 & f_{32} & 0 & f_{33} \end{pmatrix} \Delta B = \begin{pmatrix} 0 & 0 & 0 \\ f_{14} & f_{15} & f_{16} \\ 0 & 0 & 0 \\ f_{24} & f_{25} & f_{26} \\ 0 & 0 & 0 \\ f_{34} & f_{35} & f_{36} \end{pmatrix} \quad (40)$$

which is reasonable as it matches the model structure (20).

The initial condition zone matrix  $U$  has been set as a block-diagonal matrix with  $\pi/6$  rad in the angular position entries and  $\pi$  rad/s in the speed ones.

### 6.1 Robust linear controller

Solving (14), in total 8 controller gains have been obtained, yielding what it would be a standard PDC TS controller. However, the gains were virtually identical, indicating that a robust linear controller, instead of a robust PDC controller, can be used.

The fact that a TS controller does not improve over a robust linear one in most mechanical systems can be explained based on passivity ideas and the spring-damper analogy of feeding back position and speed: indeed, in a *collocated* mechanical system with *linear* actuator a high-gain PD controller will always dissipate mechanical energy (J.-J.E. Slotine, 1991; Petersen and Lanzon, 2010) and, hence, stabilise the system. So, unsurprisingly, the TS-PDC LMIs found that gain changes for each of the models did not improve the obtained worst-case cost bound.

From the above considerations, solving (14) again, considering  $Y_j = Y$ , i.e. reducing the PDC gains to a single shared linear one, the non-fuzzy robust linear controller in (41) is obtained:

$$K_{RL} = \begin{pmatrix} 108.88 & 30.06 & 0 & 0 & 0 & 0 \\ 0 & 0 & 108.88 & 30.06 & 0 & 0 \\ 0 & 0 & 0 & 0 & 181.12 & 45.92 \end{pmatrix} \quad (41)$$

Note that the resulting controller is decoupled because the original model (19) is also decoupled, i.e., there is no nominal cross-talk between actuator channels (the chosen uncertainty structure (40) allows for a limited amount of unmodelled coupling, anyway). Actuator decoupling and linearisation was done by solving (18) because inverting a known nonlinearity in the actuator side reduces the complexity of the resulting controller and, furthermore, avoided multiplying by 16 the number of rules (indeed, introducing a TS model of  $V_1^2, V_2^2, V_3^2, V_4^2$  would have led to a 128-rule model... which is rather involved and impractical).

## 6.2 Linear controller (linearised model)

This gain is computed by solving the matrix inequality (14), similarly to the TS controller design, but using only one model: the linearisation at the origin. Hence, the linear controller uses only one controller gain and one model whereas the TS/robust linear ones use eight eight models. The resulting linear controller gain matrix, with the same design parameters and uncertainty description, is given in (42).

$$K_{LC} = \begin{pmatrix} 94.79 & 25.91 & 0 & 0 & 0 & 0 \\ 0 & 0 & 94.79 & 25.91 & 0 & 0 \\ 0 & 0 & 0 & 0 & 181.46 & 45.17 \end{pmatrix} \quad (42)$$

The obtained guaranteed-cost performance bounds are 1057 for the linear robust controller and 1006 for the linear controller. As in the observer case, the linearised model obtains a theoretically slightly better performance, because there is no nonlinearity to compensate for so controlling seems “easier”. However, experiments in next section show that the linearised controller’s performance is actually worse than the robust/TS one when faced with the actual nonlinearities.

Note also that the gain in the yaw coordinates are the same in the TS/Robust controller and in the linearised one because the yaw dynamics is linear due to the quadrotor symmetry  $I_{xyz} = 0$ .

## 6.3 Propeller feedforward linearization

The designed controllers provide the transformed inputs in (18), thus, there are four squared voltages to be computed from three torque commands. As (18) in matrix form is:

$$\begin{pmatrix} u_1 \\ u_2 \\ u_3 \end{pmatrix} = \begin{pmatrix} 0 & \frac{bIK_v^2}{I_{xx}} & 0 & -\frac{bIK_v^2}{I_{xx}} \\ -\frac{bIK_v^2}{I_{yy}} & 0 & \frac{bIK_v^2}{I_{yy}} & 0 \\ \frac{dK_v^2}{I_{zz}} & -\frac{dK_v^2}{I_{zz}} & \frac{dK_v^2}{I_{zz}} & -\frac{dK_v^2}{I_{zz}} \end{pmatrix} \begin{pmatrix} V_1^2 \\ V_2^2 \\ V_3^2 \\ V_4^2 \end{pmatrix} \quad (43)$$

the pseudo-inverse of the matrix is used to obtain the voltages that minimise  $\sum_{i=1}^4 V_i^4$ . Note that there is no problem in obtaining a negative solution for any  $V_i^2$  (see footnote 1). Such pseudo-inverse actually obtains the intuitively expected actions: to increase  $u_1$ , increase  $V_2$  and decrease  $V_4$  in the same amount; to increase  $u_2$  increase  $V_3$  and decrease  $V_1$  in the same amount; to increase  $u_3$  increase  $V_1$  and  $V_3$  and decrease  $V_2$  and  $V_4$ , all in the same amount (note that the yaw action  $u_3$  is the only one that will produce a variation in the gyroscopic effect  $u_g$ ).

## 7. EXPERIMENTAL RESULTS

In this section, an experimental comparison of the linear and fuzzy observers and controllers discussed in previous sections is performed in order to assess the suitability of the TS approach in the control of these types of electromechanical systems.

The discussion is divided in two subsections: the first one will discuss only observer performance, with a preliminary stabilising standard LQR controller; the second one will discuss the performance obtained when closing the loop with the TS controller and observer. The experiment setups in each case will be different:

- The experiments with only the observer design show the capacity of the observer to estimate the states, being, at first, near the linearisation point and, then, far away from the linearisation point.

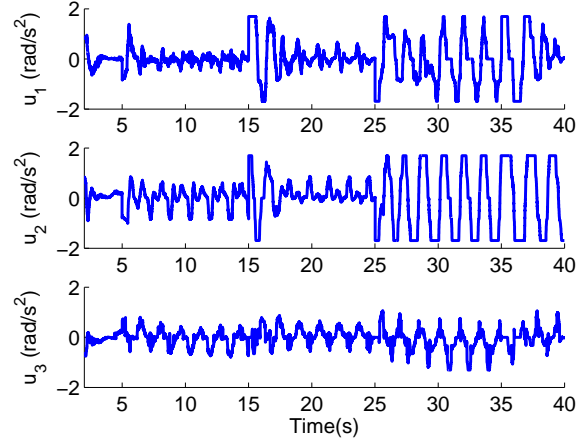


Figure 2. Experiment 1. Input data of the platform

- The experiments with the observer and the controller design show the performance of the system trying to reach the designed operating point from a nonzero initial condition.

### 7.1 Observer-only Experiments

As the open-loop system is (marginally) unstable, an LQR controller, designed on the linearised system, was implemented to stabilise the closed-loop. Inputs to the controller were the angular position (roll, pitch, yaw) and computed velocities. Note that controller details and performance are not relevant, as the system will actually be intentionally excited to leave the operating point.

Input-output data have been generated by inserting sinusoidal and step reference signals to this basic stabilizing loop.

As there is no direct access to the actual quadrotor state variables, a noncausal zero-phase filter (using command `filtfilt` in Matlab<sup>®</sup> with  $0.5/(1 - 0.5z^{-1})$  in forward and reverse time, plus numerical differentiation with the zero-phase filter  $(z - z^{-1})/(2T_s)$  in the speed coordinates) has been used to compute (off-line) a reference “real” value of speeds from the actual position measurements. The results given by the Takagi-Sugeno and linear observers have been compared to the results of this non-causal filter to compute the (approximate) error.

During the initial five seconds of excitation, the system reaches roughly a constant position (no input excitation applied) close to the linearization point.

Later, with the objective of validating the TS observer, the system has been subjected to an excitation achieving large enough angular speeds for the nonlinear terms to be significant. Hence, a sinusoidal excitation was introduced in  $\psi$  from second 5 till 40 and a reference in  $\theta$  and  $\phi$  changes every 5 seconds from 10 to  $-10$  degrees.

The input-output data collected appear in Figures 3 and 2. This data confirms that the system states satisfy the bounds from Section 3.

Note that the position estimates are actually very precise as a direct low-noise encoder output is available, so they are not shown in the figures. As intuitively expected, speed estimation is less precise and the differences between the observer alternatives in the speed case will be discussed below. The estimation

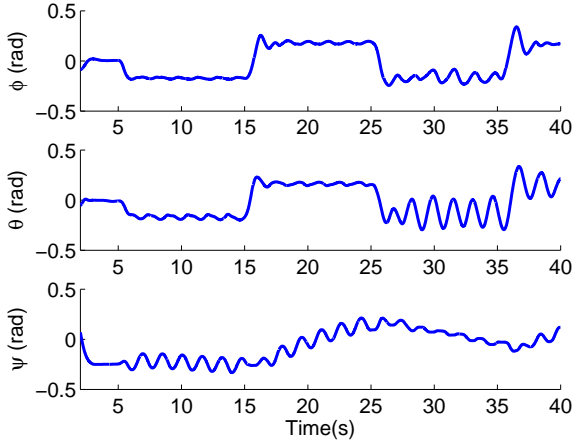


Figure 3. Experiment 1. Measurement (output) data of the platform

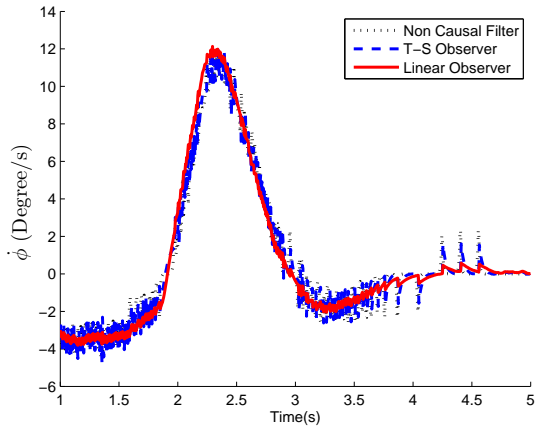


Figure 4. Experiment 1. Zoom in the time space [1 5]s

results for the noncausal filter and the Takagi-Sugeno and linear observers are detailed below.

*Low-excitation performance.* Figure 4 shows four seconds in the initial phase of the experiment, when there is no yaw excitation. It can be seen that the three observers estimate the velocity in a similar way, possibly because the linearized model is reasonably valid. In fact, the TS observer seems slightly noisier.

*High-excitation performance.* Figure 5, a zoom in of the experiment in a zone where there was a  $\psi$  excitation and reference change in  $\phi$  and  $\theta$  (from 33 to 38 seconds), shows a clear difference between the estimations of the different observers.

To have a better understanding of the estimation accuracy, the Integral Squared Error (ISE) of the estimation error (as compared to the non causal filter output) has been computed, and the result is presented in Figure 6.

Figure 6 shows that although in the first seconds the linear observer has slightly less error than the TS, when the non-linear terms (exciting with sinusoidal  $\psi$  and reference changes) affect the system, the linear observer error increases significantly. The ISE of the attitude of the quadrotor is shown in Table 2. It is clear that the error of the linear observer is larger than the error in the TS when the operating range is wider.

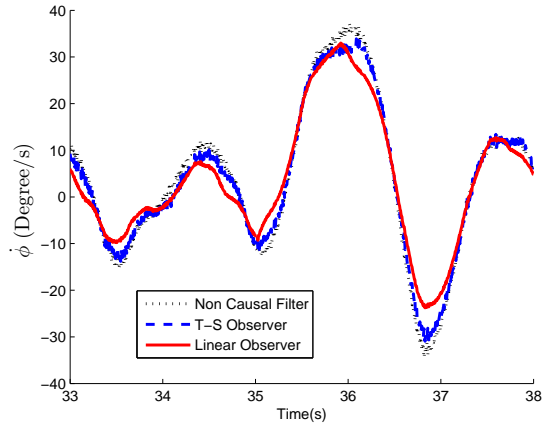


Figure 5. Experiment 1. Zoom in the time space [33 38]s

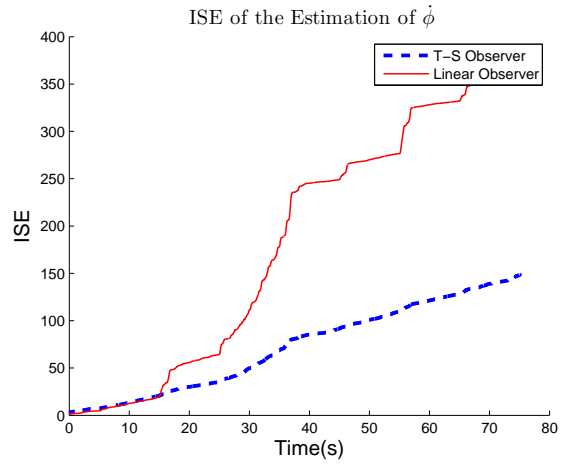


Figure 6. Experiment 1. ISE of  $\dot{\phi}$  coordinate: linear observer (solid) and TS observer (dashed)

Table 2. Exp. 1: Final ISE of attitude estimation

error	ISE TS obs.	ISE Linear obs.
pitch speed $\dot{\phi}$	148.6471	360.7385
roll speed $\dot{\theta}$	533.3477	858.5370
yaw speed $\dot{\psi}$	535.5539	1175.7

In summary, the experiment confirms that a TS observer can significantly improve estimations over an equivalent design on the linearized model when the nonlinearities in the quadrotor model have a relevant effect (i.e., when moving at high angular speeds), even if performance is roughly similar close to the linearization point at low speed (initial phase of the experiment).

## 7.2 Closed-loop TS control experiments

This section presents the results of three closed-loop experiments. The three of them start in the same position, far away of the linearization point; all of them try to drive the system to the linearization point optimizing a bound on the quadratic cost index, as discussed in previous sections.

These three experiments are set as follows:

- (1) Linear controller & linear observer, designed for the linearized model.
- (2) Linearised controller & TS observer.

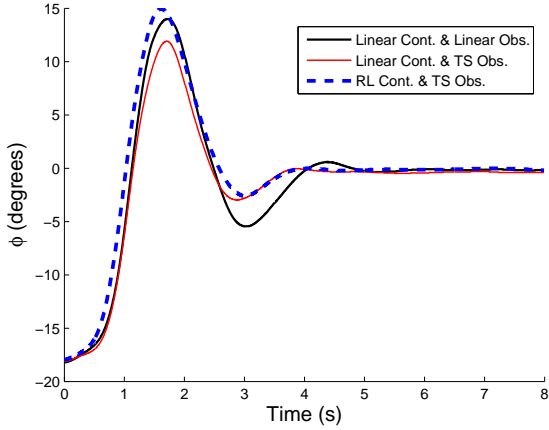


Figure 7. Closed-loop experiments. Results of the three experiments in roll

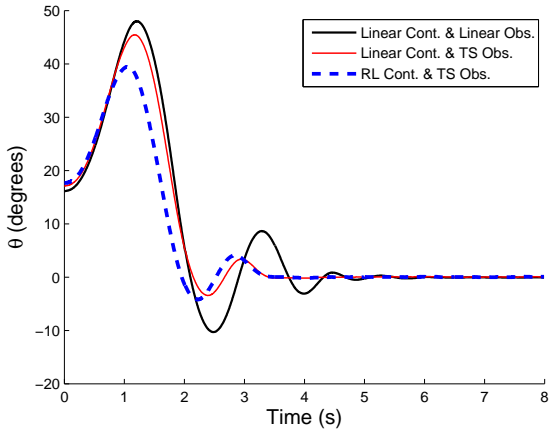


Figure 8. Closed-loop experiments. Results of the three experiments in pitch

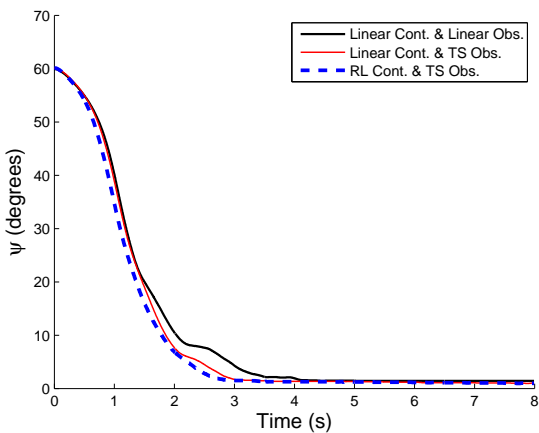


Figure 9. Closed-loop experiments. Results of the three experiments in yaw

### (3) TS (actually robust linear) controller + TS observer

The three experiments start with their 3 degrees of freedom situated at  $-18^\circ$  in roll,  $17^\circ$  in pitch and  $60^\circ$  in yaw. Their objective is to return to the equilibrium position given by  $x = 0$ .

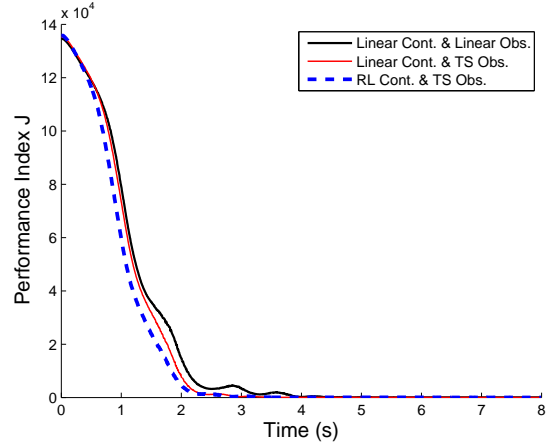


Figure 10. Closed-loop experiments. Instantaneous performance index in the experiments (total cost in Table 3 is the integral)

The time responses are shown in Figures 7, 8, and 9 for the three angular coordinates.

The actually achieved values of the objective performance index, see (12), is shown in Figure 10 (at each time instant) and Table 3 (final sum).

Table 3. Performance Index (integral)

Controller	Observer	Quadratic cost $J_t$
Linearised	Linearised	3.8797e+003
Linearised	Takagi-Sugeno	3.5264e+003
Robust Linear	Takagi-Sugeno	3.2948e+003

As Table 3 shows, the experimentally achieved transient performance index improvement with the robust+TS strategy is approximately 15% better than the linear design, and 7% better than the linearised state feedback with TS observer.

## 8. CONCLUSIONS

In this work, an LMI-based Takagi-Sugeno nonlinear observer for attitude and rotational speed estimation and a controller have been designed for an uncertain fuzzy TS model of a 3DoF quadrotor. The paper has presented a systematic methodology in order to accomplish such designs in an application framework.

The experimental results presented show that a more accurate state estimation is obtained with the TS observer (when the operating range is far away from the point of linearization) than with a similarly-designed classical linear observer. Also, a better performance is obtained when the loop is closed with such an observer and a controller designed for the TS plant model, in terms of a user-defined quadratic cost index. The controller, however, is actually a robust linear one, intuitively expected from passivity considerations: nonlinearly changing gains are not of any advantage in the worst-case guaranteed cost setting here discussed.

In this way, a realistic application of fuzzy theory has been developed in detail. The advantages of the proposed fuzzy TS modeling, observer and controller design framework over alternative (classical linearized models) strategies are experimentally confirmed in a nonlinear mechanical process.

## REFERENCES

- Abdelazim, T. and Malik, O.P. (2005). Identification of nonlinear systems by Takagi-Sugeno fuzzy logic grey box modeling for real-time control. *Control Engineering Practice*, 13(12), 1489-1498.
- Ariño, C., Pérez, E., and Sala, A. (2010). Guaranteed cost control analysis and iterative design for constrained Takagi-Sugeno systems. *Engineering Applications of Artificial Intelligence*, 23(8), 1420-1427.
- Benhadj, N. and Rotella, F. (1995). State observer design for a class of nonlinear system. *Journal of Systems Analysis*, 17, 265-277.
- Bergsten, P., Palm, R., and Driankov, D. (2002). Observers for Takagi-Sugeno fuzzy systems. *IEEE Transactions on Systems, Man and Cybernetics, Part B*, 32(1), 114-121.
- Bergsten, P. (2001). *Observers and Controllers for Takagi-Sugeno Fuzzy Systems*. Ph.D. thesis, Örebro University, Sweden.
- Bouabdallah, S. (2007). *Design and control of quadrotors with application to autonomous flying*. Ph.D. thesis, Federal Polytechnic School of Lausanne.
- Boyd, S., El Ghaoui, L., Feron, E., and Balakrishnan, V. (1994). *Linear matrix inequalities in system and control theory*, volume 15. Society for Industrial Mathematics.
- Dong, J. and Yang, G. (2007). Static output feedback control synthesis for discrete-time ts fuzzy systems. *International Journal of Control Automation and Systems*, 5(3), 349.
- Feng, G. (2006). A survey on analysis and design of model-based fuzzy control systems. *Fuzzy Systems, IEEE Transactions on*, 14(5), 676-697.
- Guelton, K., Jabri, D., Manamanni, N., Jaadari, A., and Chinh, C. (2012). Robust stabilization of nonlinear systems based on a switched fuzzy control law. *Journal of Control Engineering and Applied Informatics*, 14(2), 40-49.
- Guerra, T., Kruszewski, A., Vermeiren, L., and Tirmant, H. (2006). Conditions of output stabilization for nonlinear models in the Takagi-Sugeno's form. *Fuzzy Sets and Systems*, 157(9), 1248-1259.
- Hidayat, Z., Lendek, Zs., Babuška, R., and De Schutter, B. (2010). Fuzzy observer for state estimation of the METANET traffic model. In *Proceedings of the 13th International IEEE Conference on Intelligent Transportation Systems*, 19-24. Madeira, Portugal.
- J.-J.E. Slotine, W.L. (1991). *Applied Nonlinear Control*. Prentice-Hall, Englewood Cliffs, NJ.
- Lee, H.J., Park, J.B., and Chen, G. (2001). Robust fuzzy control of nonlinear systems with parametric uncertainties. *IEEE Trans. on Fuzzy System*, 9(2), 369-372.
- Lendek, r., Berna, A., Guzmán-Giménez, J., Sala, A., and Garcia, P. (2011). Application of Takagi-Sugeno observers for state estimation in a quadrotor. 7530-7535.
- Lendek, Zs., Babuska, R., and De Schutter, B. (2010a). Stability bounds for fuzzy estimation and control. *Journal of Control Engineering and Applied Informatics*, 12(3), 3-12.
- Lendek, Zs., Babuška, R., and De Schutter, B. (2009). Stability of cascaded fuzzy systems and observers. *IEEE Transactions on Fuzzy Systems*, 17(3), 641-653.
- Lendek, Zs., Babuška, R., and De Schutter, B. (2010b). Fuzzy models and observers for freeway traffic state tracking. In *Proceedings of the American Control Conference*, 2278-2283. Baltimore, MD, USA.
- Lendek, Zs., Guerra, T., and Babuska, R. (2010c). On non-PDC local observers for ts fuzzy systems. In *Fuzzy Systems (FUZZ)*, 2010 IEEE International Conference on, 1-7. IEEE.
- Lendek, Zs., Guerra, T., Babuška, R., and De Schutter, B. (2010d). *Stability analysis and nonlinear observer design using Takagi-Sugeno fuzzy models*. Springer-Verlag Germany.
- Lendek, Zs., Lauber, J., Guerra, T.M., Babuška, R., and De Schutter, B. (2010e). Adaptive observers for TS fuzzy systems with unknown polynomial inputs. *Fuzzy Sets and Systems*, 161(15), 2043-2065.
- Liu, J. (2007). On-line soft sensor for polyethylene process with multiple production grades. *Control Engineering Practice*, 15(7), 769-778.
- Marcu, E. (2011). Fuzzy logic approach in real-time UAV control. *Journal of Control Engineering and Applied Informatics*, 13(1), 12-17.
- Marx, B., Koenig, D., and Ragot, J. (2007). Design of observers for Takagi-Sugeno descriptor systems with unknown inputs and application to fault diagnosis. *IET Control Theory and Applications*, 1(5), 1487-1495.
- Ohtake, H., Tanaka, K., and Wang, H. (2001). Fuzzy modeling via sector nonlinearity concept. In *Joint 9th IFSA World Congress and 20th NAFIPS International Conference*, 127-132. Vancouver, Canada.
- Palm, R. and Bergsten, P. (2000). Sliding mode observer for a Takagi-Sugeno fuzzy system. In *Proceedings of the 9th IEEE International Conference on Fuzzy Systems*, volume 2, 665-670. San Antonio, Texas.
- Petersen, I. and Lanzon, A. (2010). Feedback control of negative-imaginary systems. *Control Systems Magazine, IEEE*, 30(5), 54-72.
- Quanser (2011). 3d hover system, viewed 27 July 2011. [http://www.quanser.com/english/downloads/products/3DOF\\_Hover.pdf](http://www.quanser.com/english/downloads/products/3DOF_Hover.pdf).
- Sala, A. (2009). On the conservativeness of fuzzy and fuzzy-polynomial control of nonlinear systems. *Annual Reviews in Control*, 33(1), 48-58.
- Sala, A., Guerra, T., and Babuska, R. (2005). Perspectives of fuzzy systems and control. *Fuzzy Sets and Systems*, 156(3), 432-444.
- Skogestad, S. and Postlethwaite, I. (2007). *Multivariable feedback control: analysis and design*, volume 2. Wiley.
- Takagi, T. and Sugeno, M. (1985). Fuzzy identification of systems and its applications to modelling and control. *IEEE Transactions on System Man and Cybernetics*, 15(1), 116-132.
- Tanaka, K., Ikeda, T., and Wang, H. (1998). Fuzzy regulators and fuzzy observers: relaxed stability conditions and lmi-based designs. *IEEE Trans. on Fuzzy System*, 6, 250-265.
- Tanaka, K., Ohtake, H., and Wang, H. (2009). Guaranteed cost control of polynomial fuzzy systems via a sum of squares approach. *IEEE Transactions on Systems, Man, and Cybernetics, Part B: Cybernetics*, 39(2), 561-567.
- Tanaka, K. and Wang, H.O. (2001). *Fuzzy Control System Design and Analysis: A Linear Matrix Inequality Approach*. John Wiley & Sons, New York, NY, USA.
- Tanaka, K., Ohtake, H., Seo, T., and Wang, H.O. (2011). An SOS-based observer design for polynomial fuzzy systems. In *Proceedings of the 2011 American Control Conference*, 4953-4958. San Francisco, CA.
- Wu, H. and Cai, K. (2004).  $H_2$  guaranteed cost fuzzy control for uncertain nonlinear systems via linear matrix inequalities. *Fuzzy Sets and Systems*, 148(3), 411-429.
- Wu, H.N. and Cai, K.Y. (2006).  $H_2$  guaranteed cost fuzzy control design for discrete-time nonlinear systems with pa-

parameter uncertainty. *Automatica*, 42(7), 1183–1188.  
Zhang, X. and Zeng, M. (2012). Multi-objective control of spacecraft attitude maneuver based on Takagi-Sugeno fuzzy model. *Journal of Control Engineering and Applied Informatics*, 14(1), 31–36.

#### Appendix A. OBTAINING THE BOUND OF THE OBSERVER MODEL MISMATCH

In this appendix, the process to compute  $\mu$  in expressions (25) and (26) is developed. First of all, a decomposition of the vertex matrices  $A_i$  is considered:

$$A_i = A_c + A_{i\rho} \quad (\text{A.1})$$

with  $A_{i\rho}$  being understood as the “non-linear part” of the  $\sum h_i A_i$  matrix, and  $A_c$  being a possibly arbitrary constant matrix which can be understood as the “linear part”. Considering now (24), the error term can be rewritten as:

$$\sum_{i=1}^r (h_i(\rho[k]) - h_i(\hat{\rho}[k])) A_i x[k] = \sum_{i=1}^r (h_i(\rho[k]) - h_i(\hat{\rho}[k])) A_{i\rho} x[k] \quad (\text{A.2})$$

because  $\sum_{i=1}^r (h_i(\rho[k]) - h_i(\hat{\rho}[k])) A_c = 0$ .

Hence, in order to prove (25)

$$\left\| \sum_{i=1}^r (h_i(\rho[k]) - h_i(\hat{\rho}[k])) A_{i\rho} x[k] \right\| \leq \mu \|e[k]\| \quad (\text{A.3})$$

Applying the submultiplicative norm inequality, the last expression can be rewritten as:

$$\sum_{i=1}^r \|(h_i(\rho[k]) - h_i(\hat{\rho}[k]))\| \cdot \|A_{i\rho} x[k]\| \leq \mu \|e[k]\| \quad (\text{A.4})$$

In the observer problems in consideration,  $\rho \equiv x$ . Also  $\|(h_i(x[k]) - h_i(\hat{x}[k]))\| \leq \max_{x \in \Omega} \left( \left\| \frac{\delta h_i(x[k])}{\delta x} \right\| \|x[k] - \hat{x}[k]\| \right)$ , where  $\Omega$  is the region of interest where the TS system is equivalent to the nonlinear system. Hence, as  $\|x[k] - \hat{x}[k]\| = \|e[k]\|$ ,

(A.4) can be rewritten as:

$$\left( \sum_{i=1}^r \max_{x \in \Omega} \left\| \frac{\delta h_i(x[k])}{\delta x} \right\| \cdot \|A_{i\rho} x[k]\| \right) \|e[k]\| \leq \mu \|e[k]\| \quad (\text{A.5})$$

which is fulfilled for any  $\mu$  such that:

$$\sum_{i=1}^r \max_{x \in \Omega} \left\| \frac{\delta h_i(x[k])}{\delta x} \right\| \cdot \|A_{i\rho} x[k]\| \leq \mu \quad (\text{A.6})$$

being the left-hand side computable from the knowledge of  $\Omega$ ,  $h$  and  $A_i$ .

**Quadrotor case:** Knowing that, for the particular quadrotor model:

$$\begin{aligned} \left\| \max_{x \in \Omega} \left( \frac{\delta h_i(x[k])}{\delta x} \right) \right\| &= \left\| \left( 0, \frac{1}{2\dot{\phi}_{max}}, 0, \frac{1}{2\dot{\theta}_{max}}, 0, 0 \right) \right\| = \\ &= \sqrt{\left( \frac{1}{2\dot{\phi}_{max}} \right)^2 + \left( \frac{1}{2\dot{\theta}_{max}} \right)^2} \end{aligned} \quad (\text{A.7})$$

the expression of  $\mu$  becomes:

$$\sqrt{\left( \frac{1}{2\dot{\phi}_{max}} \right)^2 + \left( \frac{1}{2\dot{\theta}_{max}} \right)^2} \sum_{i=1}^r (\|A_{i\rho} x[k]\|) \leq \mu \quad (\text{A.8})$$

To obtain a bound for  $\|A_{i\rho} x[k]\|$ , for  $x[k]$  ranging in a known hypercube by assumption, an LMI problem can be developed via S-procedure by minimizing  $\gamma$  subject to

$$\gamma - x^T A_{i\rho}^T A_{i\rho} x > 0 \quad (\text{A.9})$$

where the above inequality is required to hold for those  $x$  for which the  $n$  conditions below are true:

$$x^T D_i^T D_i x < 1 \quad i = 1, \dots, n \quad (\text{A.10})$$

being  $n$  the number of states of the model, and the (rank 1) matrices  $D_i$  being:

$$\begin{aligned} D_1 &= \text{blkdiag}(1/(\dot{\phi}_{max}), 0, 0, 0, 0, 0); \\ D_2 &= \text{blkdiag}(0, 1/(\dot{\phi}_{max}), 0, 0, 0, 0); \\ D_3 &= \text{blkdiag}(0, 0, 1/(\dot{\theta}_{max}), 0, 0, 0); \\ D_4 &= \text{blkdiag}(0, 0, 0, 1/(\dot{\theta}_{max}), 0, 0); \\ D_5 &= \text{blkdiag}(0, 0, 0, 0, 1/(\psi_{max}), 0); \\ D_6 &= \text{blkdiag}(0, 0, 0, 0, 0, 1/(\dot{\psi}_{max})); \end{aligned} \quad (\text{A.11})$$

The result is the LMI problem presented in (A.12) below, where  $\gamma$  should be minimized and  $\tau_i$  are the KKT multipliers arising from S-procedure:

$$\begin{aligned} \gamma - \sum_{i=1}^n \tau_i &> 0; \\ -A_{i\rho}^T A_{i\rho} + \sum_{i=1}^n \tau_i D_i^T D_i &> 0; \end{aligned} \quad (\text{A.12})$$

Substituting the result of (A.12) in (A.8), the final expression of  $\mu$  is:

$$\mu = \sqrt{\left( \frac{1}{2\dot{\phi}_{max}} \right)^2 + \left( \frac{1}{2\dot{\theta}_{max}} \right)^2} \sqrt{\gamma} \quad (\text{A.13})$$